PROPERTIES OF NB THIN FILMS AND THEIR APPLICATION FOR DIFFUSION-COOLED HOT-ELECTRON BOLOMETER

M. Frommberger, F. Mattiocco, P. Sabon, M. Schicke, K.F. Schuster

Insitut de Radio Astronomie Millimétrique
300 rue de la Piscine, Domaine Universitaire Grenoble
38406 St. Martin d'Hères, France

O. Laborde

Centre de Recherches sur les Très Basses Températures
25 Avenue des Martyrs
38042 Grenoble, France

ABSTRACT

The performance of hot electron bolometer mixer devices made out of superconducting thin films critically depends on film quality. We discuss various deposition conditions for Nb films and present their properties for a wide thickness range. The obtained film parameters allow to predict the characteristics of our actual devices. We also shortly present a new fabrication process for Nb diffusion cooled hot electron bolometer mixers.

I. INTRODUCTION

Nb diffusion-cooled hot electron bolometer (HEB) mixers offer very competitive performance up to several THz. Although many promising mixer results have been presented little has been published about the necessary thin film qualities and the related processing problems [1, 25].

The difficulty in fabrication of Nb HEBs originates not only from the requirement of very high resolution lithography but also from the need of high quality Nb thin films and their protection throughout the processing steps.

In a first part we report on investigations on Nb thin films in a thickness range from 2 to 80 nm. Different characterisation methods like dc-measurements, x-ray diffraction (XRD) and atomic force microscopy (AFM) were applied. In a second part we

present a new processing sequence for Nb HEBs and high frequency measurements carried out with such devices.
We derived the time constants from thin film characterisations and compared them with values obtained by high frequency measurements.

II. THIN FILM PREPARATION

For device fabrication it is essential to obtain a high reproducibility in film thickness. As a low deposition rate is one way to improve thickness calibration we started out with a low sputter power (~ 0.5 nm/s for 200 W). The Nb thin film samples have been produced on 2" fused quartz substrates which underwent a rigorous ultrasonic cleaning in acetone and propanol. Such substrates should also serve as a good reference for silicon substrates with native oxide.
The background pressure in the sputterer chamber is about 2×10^{-8} mbar and the films were deposited by dc-magnetron sputtering at 2 Pa after Ar-plasma RF cleaning of the substrate. No active substrate heating was applied during film deposition.
Figure II.1a shows an AFM image of a 120 nm thick Nb film sputtered with 200 W at 2 Pa. One can observe a polycristalline film growth with a grain size of about 10 to 30 nm. In comparison, figure II.1b shows a film deposited at 730 W and 2 Pa. The observed grainsize is about 3 times larger than for 200 W.

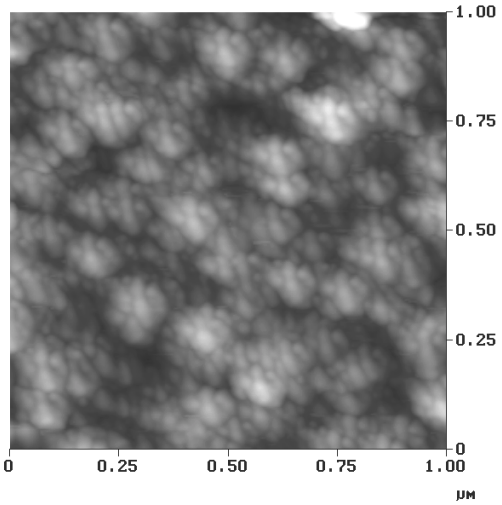

Fig. II.1a. AFM image of a 120 nm Nb film sputtered at 200 W, 2 Pa.

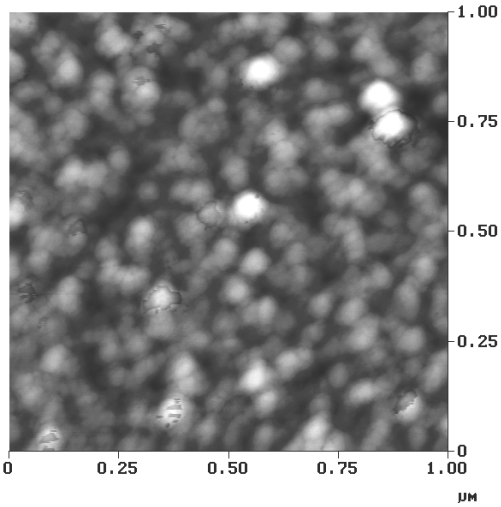

Fig. II.1b. AFM image of a 120 nm Nb film sputtered at 730 W, 2 Pa.

X-ray diffraction (XRD) measurements which were carried out in the context of stress determination gave comparable results for the crystallinity of our Nb layers [8]. Figure II.2 shows XRD curves for 120 nm Nb films sputtered at different source

powers. Depending on the sputter power we can see a clear transition from polycrystalline to quasi amorphous film growth. Best crystallinity is obtained for 800 W. The grainsizes determined by XRD were:

Power	**200 W**	**400 W**	**600 W**	**800 W**
2θ	37.682	38.789	38.549	38.468
$\mathbf{w_{fwhm}}$	1.051	0.414	0.320	0.288
grainsize	7.6 nm	27 nm	35 nm	39 nm

With decreasing power, intensity of the (110) peak is descending and the peak shifts to higher values of 2θ, due to increasing tensile stress. Below 400 W film stress becomes highly compressive.

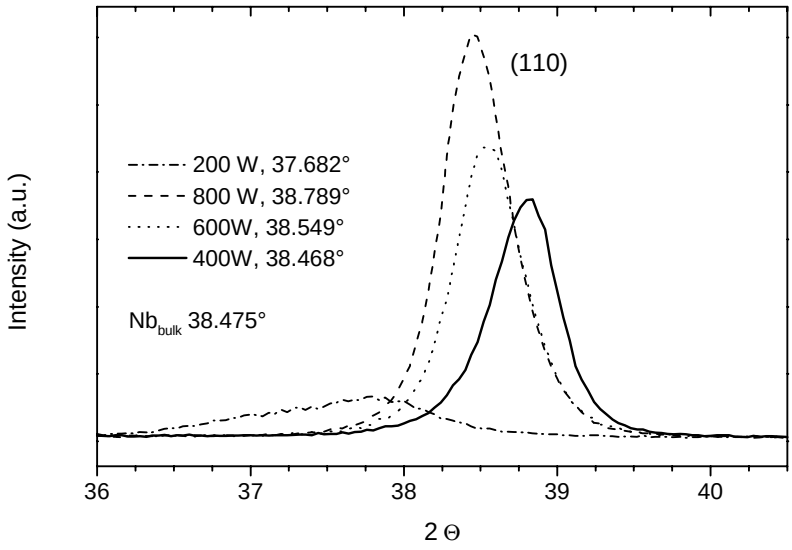

Fig. II.2. X-ray diffraction results of 120 nm Nb films sputtered at 200, 400, 600 and 800 W and 2 Pa. 2θ for the (110) peak center and for bulk Nb [19] is shown on the plot (Cu K_α).

III. ELECTRICAL THIN FILM PROPERTIES

We determined the electrical properties of our films by four point measurements on $1\,\mathrm{mm} \times 10\,\mathrm{mm}$ samples which were carried out in a dip-stick set up. The film thickness has been varied from 2 to 80 nm and verified by anodisation. The residual

resistance ratio RRR and the sheet resistance above the critical temperature T_c and their dependence on film thickness were investigated.
As can be seen in figure III.1 the sheet resistance at 10 K does not simply follow a curve proportional to the invers of the geometrical cross section for films below 20 nm.

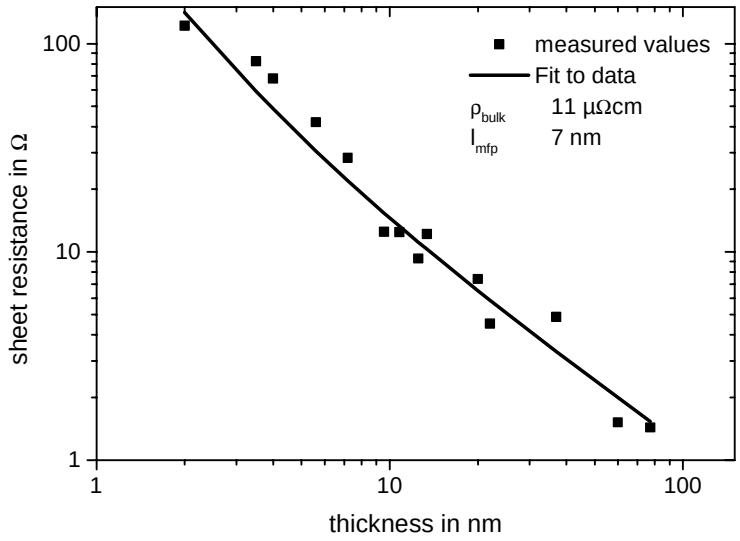

Fig. III.1. Sheet resistance at 10 K versus film thickness. The squares are our measured data, the solid line corresponds to the size effect model. The fit to our data gives a ρ_{bulk} of 11 $\mu\Omega$cm and a l_{mfp} of 7 nm for films sputtered with 200 W..

Different explications have been given in the past for the observed behavior. A thickness dependent grain size distribution could play a certain role due to interface effects. Jiang showed that weak localisation effects become important for ultra thin epitaxial films [24].
However for our films a simple size effect model taking into account the surface scattering of electrons can explain the measurement to a sufficient accuracy (see fig. III.1). The resistivity in this model is described by

$$\rho \approx \rho_{bulk} \cdot \left(1 + \frac{3}{8}\frac{l_{mfp}}{t}\right) \Rightarrow \; Rs \approx \rho_{bulk} \cdot \left(\frac{1}{t} + \frac{3}{8}\frac{l_{mfp}}{t^2}\right)$$

which can be derived from kinetic theory arguments (*Rs* is the sheet resistance, l_{mfp} the electron mean free path, *t* the film thickness and ρ_{bulk} the bulk resistivity at 10 K) [2, 23]. This formula should be a reasonable first approximation for a thin film containing a free electron gas in which electrons striking the sample surface are scattered completely diffusely. In our case the surfaces are given by the thin film-

substrate interface and the NbOxide surface layer. Identification of the electron mean free path l_{mfp} found by the size effect model with a typical grain size gives good agreement with XRD and AFM measurements.

Figure III.2 shows the dependence of the critical temperature on the film thickness. To explain our data, we employ a proximity effect model. For single-crystalline Nb films Yoshii et al. [11] achieved good agreement with such a model considering a system of a superconducting layer (thickness d) and a normal-metal layer (thickness a) to describe the depression of T_c with decreasing film thickness.

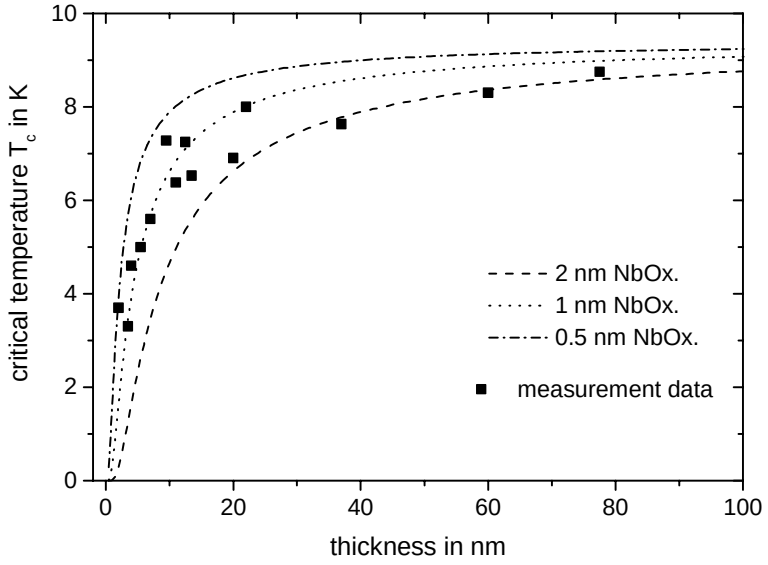

Fig. III.2. Critical temperature T_c versus film thickness. The curves are calculations assuming a NbOxide layer of 0.5 nm, 1 nm, 2 nm respectively, the squares are the measurement values.

The graphs in fig. II.2 show the calculation of T_c versus film thickness for different NbOxide layer thicknesses, following their formula

$$T_c = T_{c0}\left(\frac{1.13\cdot\Theta_D}{T_{c0}}\right)^{-[N_N(0)/N_s(0)](a/d)}$$

which has originally been proposed by McMillan [12, 14]. Here T_{c0} is the transition temperature of the bulk (9.3 K), Θ_D the Debye temperature of the superconducting layer (Nb, 275 K), and $N_N(0)$ and $N_S(0)$ are the density of states for normal and superconducting layers respectively [13].

As the McMillan formula is only adequate for the dirty limit case only films below 20 nm will be correctly described. From figure III.2 we can conclude an oxide thickness of 1 nm, a value which is in good agreement with results from ellipsometry for films exposed for some minutes to ambient air [8, 20].

IV. DEVICE FABRICATION

Existing diffusion-cooled hot-electron bolometer devices consist out of a sufficently short and thin superconducting microbridge connected to Au pads which serve as heat sinks [3]. The device impedance must be matched to a given source impedance, typically in the range of 25 to 70 Ω.
In comparison to the HEB fabrication process used by the JPL group [17], we present a simplified process, avoiding the chlorine containing gas mixture (freon) and the unselective reactive ion etching (RIE) step for the final bridge definition. The actual IRAM diffusion-cooled Nb HEB devices are fabricated in the following steps:
After an overall deposition of a 10-20 nm Nb film and a 10 nm Au oxidation-protection layer on a 2" fused quartz substrate we define the antenna and filter structure by photolithography.
To define the lateral dimensions of the microbridge we use Ebeam lithography. In a first step we fix the microbridge length by defining the Au cooling pads by a double PMMA layer (950K/50K) lift-off process. Here the 10 nm Au layer allows a high pre-bake temperature for the PMMA layers without destroying the Nb film. Such a high bake temperature helps to avoid intermixing of the two layers and stabilizes the resist profile for a better lift-off. Afterwards we remove the Au protection with an argon plasma. In a second Ebeam step we generate a lift-off pattern by which a thin Al strip is defined. This Al strip is used as a selective etch mask. We remove the surrounding Nb by reactive ion etching (CF_4, O_2). The Al etch mask is removed by a strong base. Finally the substrate is diced and the individual devices are characterised by a dc-measurement.

V. RF- AND IF- MEASUREMENTS

To measure the RF matching between antenna and detector, we tested our HEB mixer as a direct detector on a Fourier Transform Spectrometer (FTS) using a chopped blackbody source (fig. V.1). As the antenna was designed for high impedance NbN HEBs, the Nb HEBs (< 50 Ω) are strongly mismatched.
Despite this mismatch one can clearly see the water vapour absorption lines between 0.5 and 1 THz.

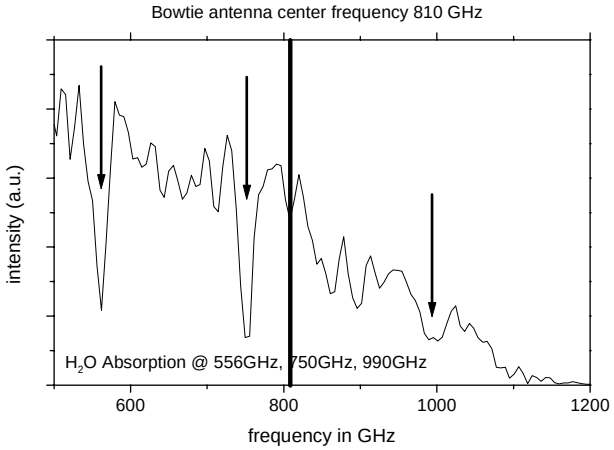

Fig. V.1 Fourier transform spectrometer measurement of a bowtie antenna with central diffusion-cooled HEB. Indicated are the water vapour absorption lines at 556, 750 and 990 GHz and the designed center frequency of the antenna at 810 GHz.

With a comparable device we performed a Y-factor measurements in the range of 800 GHz. Figure V.2. shows the pumped I(V)-curve of the device together with the conversion curves for the hot and cold load. Best mixer noise temperature was 4030 K at 2.2 K bath temperature, 798 GHz local oscillator frequency and an IF of 1.37 GHz. The impedance mismatch mentioned above and the beam splitter loss add about a factor 3 to the noise temperature.

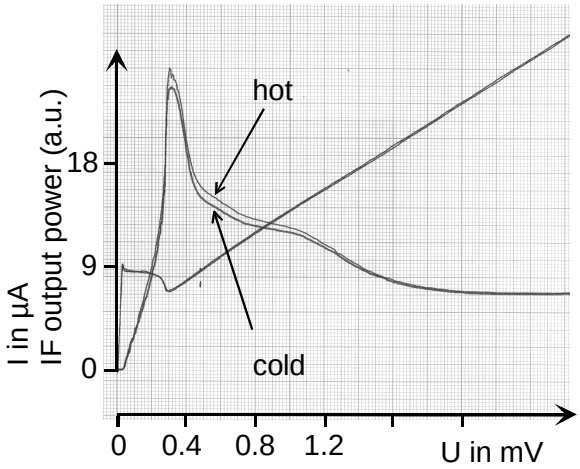

Fig.V.2 Pumped I(V)- and conversion curves for the hot and cold load at 2.2 K. The Y-factor measurement at a local oscillator frequency of 798 GHz and an intermediate frequency of 1.37 GHz gave a non corrected noise temperature of 4030 K.

For application in THz radioastronomy the IF bandwidth of the HEB mixer devices should be as high as possible.
To access the intrinsic time scales of the Nb films which determine the IF bandwidth we executed an impedance measurement similar to the procedure described by Karasik et al. [6,7]. In order to allow a rapid measurement we installed the setup in a dipstick which could be immersed in liquid helium. The measurement was done with a HP8510 network analyzer. The dc bias was directly fed over the internal bias input of the HP8510. The measurements were performed with a sweep between 500 MHz and 10 GHz and a power level of -65 dBm at the device. With a calibration scheme as described by [6] we obtained the complex impedance as plotted in Fig. V.3. The frequency dependence of the device impedance is given by [6]

$$Z(\varpi) = R \cdot \frac{1+C}{1-C} \cdot \frac{1+i\varpi\dfrac{\tau_0}{1+C}}{1+i\varpi\dfrac{\tau_0}{1-C}}$$

where C is the self heating parameter and τ_0 the electron temperature relaxation time and R the device resistance at the operating point.
The solid lines in fig. V.1 show Z(f) calculated with values obtained by a fit to ZZ^* of the measured data where τ_0 and C where the free fitting parameters.

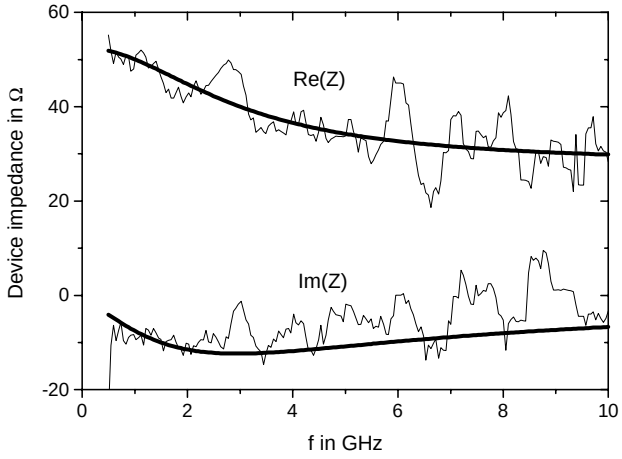

Fig. V.3. Real and imaginary part of the impedance of a diffusion-cooled Nb hot-electron bolometer over frequency. The solid lines correspond to the best fit parameters obtained by the network analyzer measurement.

From the impedance measurement one can obtain the electron temperature relaxation time τ_0 which, for diffusion-cooled Nb HEBs, is in the order of the diffusion time τ_{diff}. The diffusion time can be calculated for a given device geometry by

$$\tau_{diff} = \frac{L^2}{\pi^2 \cdot D},$$

where D is the diffusion constant [16]. We derived D from measurements of the slope of the critical magnetic field H_{c2} [5, 22] near the superconducting transition. For a 14 nm Nb film we obtained a diffusion constant of D = 2.2 cm^2/s.
The IF bandwidth is directly related with these intrinsic times via

$$\Delta f_{3dB} \approx \frac{1}{2 \cdot \pi \cdot \tau}.$$

As the electrons should thermalize before out-diffusion into the contact pads, τ_0 should be larger than the electron-electron relaxation time τ_{ee} which can be estimated out of the thin film parameters (sheet resistance Rs and T_c, see figure III.1 and III.2) by

$$\tau_{ee} \propto \left(10^8 \cdot Rs \cdot T_c\right)^{-1} \cdot s,$$

where Rs is in Ω and T_c is in K [4]. It gives an approximate number for the electron temperature relaxation length l_{ee} [9]

$$l_{ee} \approx 2 \cdot \sqrt{D \cdot \tau_{ee}}$$

which is in the order of 100 nm. For a short device the hot electrons may diffuse out of the microbridge more quickly than they interact with each other, an effect recently debated for aluminium HEBs [10, 15, 18, 21].

	thin film characterisation	**IF bandwidth measurement**
intrinsic time constants	electron diffusion time $\tau_{diff} \approx 3 \times 10^{-11}$ s	electron temperature relaxation time $\tau_0 = 3.35 \times 10^{-11}$ s
	electron electron relaxation time $\tau_{ee} \approx 1 \times 10^{-11}$ s	
IF bandwidth $\Delta f_{3dB} = \frac{1}{2\pi \cdot \tau}$	for τ_{diff} Δf_{3dB} = 5.5 GHz	for τ_0 Δf_{3dB} = 4.3 GHz

Tab. V.4. Comparison of the intrinsic time scales obtained by calculations on thin film data and the bandwidth measurement of an actual device. In both cases we assume a device length of 250 nm and an effective film thickness of 14 nm.

In Table V.4. we compare the obtained time constants. For the thin film calculations we assumed a 250 nm long HEB. Starting out with a 20 nm film deposition we assume an effective film thickness of 14 nm due to the NbOxide top layer after processing (4 nm) and the film substrate interface (2 nm) [8]. As expected, the

calculated IF frequency bandwidth is in the same order of magnitude as the experimental value and the electron temperature relaxation time is almost equal to τ_{diff}, confirming the cooling mechanism in the HEB device.

VI. CONCLUSION

Thin Nb films have been investigated in a wide thickness range. AFM as well as XRD show that using high power sputtering will significantly increase film quality.
The electrical properties of the currently used and unoptimised thin films were explained by a size effect and a proximity effect model. The results give us the possibility to predict the final high frequency characteristics of a Nb diffusion-cooled HEB for a given device geometry. We developped a simple Nb HEB process; a mixing experiment at 798 GHz was carried out on a device fabricated with this process. With an maladjusted antenna we obtained an uncorrected receiver noise temperature of 4030 K at an intermediate frequency of 1.37 GHz.. The devices showed a 3dB cut-off frequency of 4 GHz. Future devices will use improved film quality.

ACKNOWLEDGEMENT

The authors like to thank H. Rothermel (MPE Garching), F. Schäfer (MPI Bonn), J. Halbritter (FZ Karlsruhe) and D. Wilms Floet (RU Groningen) for helpfull discussions and J. Schülein (PI3 Erlangen) for the AFM measurements.

REFERENCES

[1] B.S. Karasik, A. Skalare, R.A. Wyss, W.R. McGrath, B. Bumble, H.G. LeDuc, J.B. Barner and A.W. Kleinsasser, *"Low noise and Wideband Hot-Electron Superconductive Mixers for THz Frequencies"*, 6th IEEE Int. Conf. on THz Electronics, Leeds, 1998
[2] K.L. Chopra, *Thin Film Phenomena*, New York, 1979
[3] B. Bumble, H.G. LeDuc, *"Fabrication of a Diffusion Cooled Superconducting Hot Electron Bolometer for THz Applications"*, IEEE Trans. Appl. Supercond. 7, 3560, 1997
[4] P. Santhanam, D.E. Prober, *"Inelastic electron scattering mechanisms in clean aluminium films"*, Phys. Rev. B 24 (6), 1984
[5] B.S. Karasik, K.S. Il'in, E.V. Pechen, S.I. Krasnosvobodtsev, *"Diffusion Cooling mechanism in a hot electron NbC microbolometer mixer"*, Appl. Phys. Lett. 68 (16), 1996

[6] B.S. Karasik, M.C. Gaidis, W.R. McGrath, B. Bumble, H.G. LeDuc, *"A Low Noise Superconductive Nb Hot-Electron Mixer at 2.5 THz"*, 8th Int. Symp. on Space Terahertz Technology, Harvard University, 1997
[7] C. Rösch, F. Mattiocco, K.F. Schuster, *"Development and Characterisation of NbN Phonon-Cooled Hot-Electron Bolometer Mixers at 810 GHz"*, 10th European Conference on Applied Superconductivity (EUCAS), Sitges, 1999
[8] P. Sabon, *"Optimisation et Caractérisation de films minces de niobium déposés par pulvérisation cathodique"*, memoire CNAM, 2000
[9] B.S. Karasik, A.I. Elantev, *"Analysis of the Noise Performnace of a Hot-Electron Superconducting Bolometer Mixer"*, 6th Int. Symp. on Space terahertz Technology, 1995
[10] B.S. Karasik, M.C. Gaidis, W.R. McGrath, B. Bumble, H.G. LeDuc, "Low noise in a diffusion-cooled hot-electron mixer at 2.5 THz", Appl. Phys. Lett. 71 (11), 1997
[11] K. Yoshii et al., *Superconductuvity and electrical properties in single-crystalline ultrathin Nb films grown by molecular-beam epitaxy*, Phys. Rev. B, **52** (18), 1995
[12] L.N. Cooper, *"Superconductivity in the neighborhood of metallic comtacts"*, Phys. Rev. Lett. 6 (12), 689, 1961
[13] Note that this formula is equivalent to that introduced using the de Gennes's expression of effective N(0)V [P.G. de Gennes, Rev. Mod. Phys. 36, 225 (1964)] for the interaction constant of normal layer $V_N = 0$; i.e., the normal layer does not show superconductivity at any temperature.
[14] W.L. McMillan, *Tunneling model of the super-conducting proximity effect*, Phys. Rev. **175**, No. 2, 537, 10. Nov. 1968
[15] A.D. Semenov, G.N. Gol'tsman, *"Non-thermal response of a diffusion-cooled hot-electron bolometer"*, IEEE Trans. Appl. Supercond. 9 (2), 4491, 1999
[16] B.S. Karasik, W.R. McGrath, R.A. Wyss, *"Optimal choice of material for HEB superconducting mixers"*, IEEE Trans. Appl. Supercond. 9 (2), 4213, 1999
[17] B. Bumble, H.G. LeDuc, *"Fabrication of a diffusion cooled superconducting hot electron bolometer for THz mixing applications"*, IEEE Trans. Appl. Supercond. 7, 3560, 1997
[18] A.D. Semenov, G.N. Gol'tsman, *"Nonthermal mixing mechanism in a diffusion-cooled hot-electron detector"*, J. Appl. Phys. 87 (1), 2000
[19] JCPDS - 35-0789, International Center for Diffraction Data, 1998
[20] Higher values for the NbOxide layer can be obtained by oxidation in water or by use of an activated oxygen environment, giving a maximum of 7 nm (T. Scherer, IEGI Karlsruhe)
[21] H. Pothier, S. Guéron, N.O. Birge, D. Esteve, M.H. Devoret, *"Energy distribution function of quasiparticles in mesoscopic wires"*, Phys. Rev. Lett. 79 (18), 1997
[22] E.M. Gershenzon, M.E. Gershenzon, G.N. Gol'tsman, A.M. Lyul'kin, A.D. Semenov, A.V. Sergeev, *"Electron-phonon interaction in ultrathin Nb films"*, Sov. Phys. JETP 70 (3), 1990

[23] J. Bass, K.H. Fischer, *"Size Effects"*,Condensed Matter III 15a, Landolt-Börnstein, 1982
[24] Q.D. Jiang, Y.L. Xie, W.B. Zhang, H. Gut, Z.Y. Ye, K. Wu, J.L. Zhang, C.Y. Li, D.L. Yin, *"Superconductivity and transport properties in ultrathin epitaxial single-crystal niobium films"*, J.Phys.: Condens. Matt. 2, 1990
[25] W.F.M. Ganzevles, J.R. Gao, D. Wilms Floet, G. de Lange, A.K. van Langen, L.R. Swart, T.M. Klapwijk, P.A.J. de Korte, *"Twin-Slot Antenna coupled Nb hot-electron bolometer mixers at 1 THz and 2.5 THz"*, Proceedings of the 10th International Symposium on Space Terahertz Technology, 247-261, 1999